

Overcoming the resistance of hepatocellular carcinoma to PD-1/PD-L1 inhibitor and the resultant immunosuppression by CD38 siRNA-loaded extracellular vesicles

Jun Deng^a and Hui Ke^b

^aDepartment of General Surgery, the First Affiliated Hospital of Nanchang University, Nanchang, Jiangxi, 330006, China; ^bSurgical Dressing Room, Union Hospital, Tongji Medical College, Huazhong University of Science and Technology, Wuhan, Hubei, 430022, China

ABSTRACT

Extracellular vesicles (EVs) are promising tools for drug delivery across different biological barriers. Here, we evaluated the potential of EVs-mediated delivery of CD38 siRNA on the immunosuppression of hepatocellular carcinoma (HCC). EVs were isolated from bone marrow mesenchymal stem cell culture medium and loaded with CD38 siRNA to prepare EVs/siCD38. Loss-of-function assays were conducted to investigate the biological functions of EVs/siCD38 in HCC cells. Xenograft mouse models were performed for further validation. High CD38 expression was found in HCC. EVs/siCD38 inhibited CD38 enzyme activity, decreased adenosine production, and promoted macrophage repolarization to M1 type, thus inhibiting HCC cell growth and metastasis *in vitro* as well as tumor growth in mice. Mechanistically, CD38 was upregulated in mice resistant to PD-1/PD-L1 inhibitor and EVs/siCD38 reversed the resistance of tumor to PD-1/PD-L1 inhibitor *in vivo*. Our results provide functional evidence for the use of EV-mediated delivery of CD38 siRNA to prevent immunosuppression feature of HCC.

ARTICLE HISTORY

Received 1 August 2022
Revised 23 November 2022
Accepted 23 November 2022

KEYWORDS

Hepatocellular carcinoma; resistance; CD38 siRNA; extracellular vesicles; macrophages; PD-1/PD-L1 inhibitor; immunosuppression

Introduction

Hepatocellular carcinoma (HCC) develops through a multistep procedure from liver cirrhosis to low-grade/high-grade dysplastic nodule, early-stage HCC and progressed HCC,¹ showing increasing incidence.² In China, HCC ranks the second most frequently occurring malignancy responsible for 300,000 to 400,000 death cases on an annual basis.³ Treatment strategies for HCC consist of medical, locoregional surgical therapies and immunotherapy while a strong intrinsic immune suppressive microenvironment in the liver severely compromises the treatment efficiency of HCC.^{4,5} Development of more effective therapeutic modalities against HCC should be directed at the immunosuppression of this disease.

Extracellular vesicles (EVs) are small single-membraned vesicles,⁶ and transfer of EVs as natural carriers of functional small RNA and proteins has attracted wide attention in the drug delivery due to the potential use of these vesicles for the therapeutic transfer of small interfering RNAs (siRNAs), mRNAs, microRNAs, long non-coding RNAs, peptides and synthetic drugs.^{7,8} CD38 is a multifunctional trans-membrane protein and abnormally overexpressed in various tumors, which is associated with cancer progression.⁹ CD38 gene expression is a prognostic marker in HCC related to pro-inflammatory state.^{10,11} Also, the expression of CD38 is implicated in the metastasis potentiality and a shortened survival in lung adenocarcinoma while increased CD38⁺ cells are indicative of response to immune-checkpoint blockade and superior median progression-free survival and overall survival in advanced HCC patients.^{11,12} CD38 is present on the surface

of numerous immune cells that have intensive correlation with antitumor immunity and immune resistance of tumor cells.¹³ CD38 in the tumor microenvironment reflects the response to anti-PD-1/PD-L1 immunotherapy in HCC.¹¹ Anti-PD-1/PD-L1 therapies have proved efficacy to prevent the immune evasion of tumor cells and are thus a powerful approach to a variety of cancers, including HCC.¹⁴ However, a large number of patients remain refractory to anti-PD-1/PD-L1 therapies over time, thus limiting the durability of anti-PD-1/PD-L1 therapies.¹⁵ A better understanding on the mechanisms of acquired resistance is thus a prerequisite to expand the benefit of immunotherapy for patients with HCC. This study aims to elucidate the possible mechanisms by which CD38 siRNA-loaded EVs (EVs/siCD38) reverses the resistance of HCC to PD-1/PD-L1 inhibitors in clinical sample, cell and animal experiments.

Materials and methods

In silico analysis

HCC-related mRNA expression dataset GSE84005 containing 38 HCC tissue samples was retrieved from the GEO database, along with GSE174570 containing 57 HCC tissue samples. Datasets GSE84005 and GSE174570 were merged into one profile, followed by the removal of batch effect using ComBat function of the R “sva” software package. The difference of principal component analysis before and after the removal of bath effect was shown. The correlation between all genes and PD-L1 expression was analyzed by Pearson correlation

coefficient using $|\text{correlation coefficient } R| > 0.35$ and $p < .05$ as the threshold criteria. HCC-related genes were retrieved from the CTD database using “Hepatocellular carcinoma” as the keyword and Inference Score >90 as the threshold criteria. GeneCards database was applied for retrieval of HCC- and tumor immune-related genes using “Hepatocellular carcinoma” and “Tumor immunotherapy” as the keywords and Gifts >40 as the threshold criteria. The above retrieval results were intersected using *jvenn* to identify the candidate genes, which were then imported into STRING database for PPI analysis with the species as “human”, the results of which were visualized by Cytoscape software (v3.8.2). The retrieval date was July 3rd, 2022.

Clinical tissue samples

HCC tissue and adjacent normal tissue specimens were collected from 42 patients with primary HCC (aged 41–75 years, with a mean age of 56.69 years) underwent surgery at The First Affiliated Hospital of Nanchang University from January 2012 to December 2016. None of the patients had received radiotherapy, chemotherapy, or biological therapy before surgery, and they had no history of surgical resection or metastatic disease. The basic characteristics of the patients are detailed in Supplementary Table 1. After collection, fresh tissues were frozen in liquid nitrogen for subsequent experimentations. This study was approved by the clinical Ethics Committee of The First Affiliated Hospital of Nanchang University and performed in strict accordance with the *Declaration of Helsinki*, with the informed consent obtained from all patients or their families.

Cell culture and transfection

Human normal hepatocyte cell line MIHA (CL0469, Hunan Fenghui Biotechnology Co., Ltd., Hunan, China), human HCC cell lines Huh-7 (CL-0120, Procell Life Science & Technology Co., Ltd., Wuhan, Hubei, China), HCCLM3 (CL-0278, Procell), and MHCC97-L (CL-0497, Procell) and human monocyte line THP-1 (TCHu 57, Cell Bank of Shanghai Chinese Academy of Sciences) were cultured in RPMI 1640 medium (PM150210, Procell) containing 10% fetal bovine serum (FBS), 100 U/mL penicillin and 100 U/mL streptomycin. Then, mouse liver epithelial cell line BNL 1ME A.7 R.1 (CL-0323, Procell), and mouse HCC cell line Hepa1-6 (SCSP-512, Cell Bank of Shanghai Chinese Academy of Sciences) were cultured in DMEM (PM150210, Procell) containing 10% FBS, 100 U/mL penicillin and 100 U/mL streptomycin. All cells were incubated in an incubator with 5% CO₂ at 37°C. The medium was renewed every 3 days. Upon reaching 80% confluence, cells were treated with 0.25% trypsin/EDTA for passage.

siCD38-1 and siCD38-2 recombinant lentivirus and siNC lentivirus (Shanghai GenePharma Co., Ltd., Shanghai, China; Supplementary Table 2) were prepared and titrated to 10⁹ TU/mL. HCCLM3 cells were transduced with siCD38-1, siCD38-2 and siNC for 72 h. Then, the culture medium was replaced with 4 µg/mL puromycin-containing medium, and cell culture continued for at least 14 days. The puromycin-resistant cells underwent amplification culture in 2 µg/mL puromycin-

containing medium for 9 days, and then transferred to the puromycin-free medium. Finally, HCCLM3 cells with stable knockdown of CD38-1 were obtained.

RT-qPCR

Total RNA was extracted from cells with TRIzol reagent (16096020, Thermo Fisher Scientific, Waltham, MA). The extracted RNA was reversely transcribed into cDNA using the cDNA Reverse Transcription Kit (RR047A, TaKaRa, Tokyo, Japan). RT-qPCR was completed on 50 ng/µL cDNA employing LightCycler 480 SYBR Green I Master (04707516001, Roche, Germany). The fold changes were calculated with the help of the 2^{-ΔΔCt} method with β-actin as internal reference. The primer sequences are detailed in Supplementary Table 3.

Western blot analysis

Total protein extracts were separated using 8–12% SDS gel electrophoresis and transferred onto a polyvinylidene difluoride membrane (1620177, Bio-Rad Laboratories, Hercules, CA). Next, the membrane was treated with 5% bovine serum albumin at room temperature for 1 h and then underwent overnight incubation at 4°C with primary rabbit antibodies (Abcam Inc., Cambridge, UK) against CD38 (ab108403, 1:1000), ARG1 (ab133543, 1:5000), and GAPDH (ab9485, 1:2500). The next day, the membrane was re-probed with secondary antibody HRP-labeled goat anti-rabbit IgG (ab6721, 1:5000, Abcam) at ambient temperature for 1 h. Afterward, ECL reagent (1705062, Bio-Rad) was used to visualize the results by the Image Quant LAS 4000C Gel Imager.

IHC

Paraffin sections of human HCC tissue samples and mouse tumor tissues were dewaxed, dehydrated in ascending series of alcohol and subjected to antigen retrieval in a water bath. Next, the sections were blocked with normal goat serum (C0265, Beyotime) for 20 min, and immunostained with primary rabbit antibodies to CD38 (ab216343, 1:1000, Abcam) and Ki67 (ab15580, 1:200, Abcam) at 4°C overnight and with secondary antibody of goat anti-rabbit IgG (ab6721, 1:1000, Abcam) at 37°C for 20 min. Subsequently, the sections were observed under a microscope in 5 randomly selected high-power fields from each section. The results were evaluated by an experienced pathologist. The positive rate was calculated: positive rate = positive cells/total cells.

CD38 enzymatic activity

CD38 enzymatic activity was measured using fluorimetry. In brief, each sample was lysed with cell lysis buffer containing both protease and phosphatase inhibitors (P0013, Beyotime), and centrifuged with the supernatant collected. The supernatant was then supplemented with 80 µM NAD (NAD100-RO, Sigma-Aldrich Chemical Company, St Louis, MO) as a substrate reaction. Samples were measured using a microplate reader and fluorescence was measured at 37°C,

Ex/Em = 340/460 nm, once per min for 1 h. CD38 enzymatic activity was calculated as the slope of the linear part of the fluorescence time curve.

Adenosine content detection

HCCLM3 cells were treated with siCD38 and siNC for 48 h and then with or without 100 M adenosine deaminase inhibitor EHNA (HY-103160A, MCE). At 0, 6, 12, 18 and 24 h, cell medium supernatant was collected where adenosine content was measured using fluorescent adenosine assay kit (ab211094, Abcam, or xyA349Ge, Guidechem, Shanghai, China). For the tissue samples, they were immersed in 0.4 mol/L frozen perchloric acid solution homogenate, and centrifuged at 4000 r/min for 15 min. The supernatant was harvested and centrifuged at 4000 r/min and 0°C for 15 min (5 mol/L potassium hydroxide titrated to pH = 7.0). Finally, the supernatant was collected for detection.

THP-1 cell differentiation

THP-1 cells were treated with 200 nM phorbol 12-myristate 13-acetate (PMA, P8139, Sigma-Aldrich). After 3 days, the medium was renewed with conventional medium without PMA and cells continued to culture for 2 days to generate differentiated THP-1 cells, namely the activated macrophages, which were used for subsequent experiments.

Macrophage polarization assay

Cell culture medium supernatant (siNC-TCM and siCD38-TCM) was collected after 48 h of treatment of HCCLM3 cells with siCD38 and siNC. The supernatant was added to the activated macrophages THP-1, which were collected 24 h later. RT-qPCR was used to examine the mRNA expression of the M2 macrophage markers IL-10 and ARG1 and M1 macrophages markers IL-12, iNOS, and TNF- α . Protein expression of IL-10, IL-12, iNOS, and TNF- α was determined by ELISA. Protein expression of ARG1 was determined by Western blot analysis.

ELISA

Cell culture supernatant was collected where the contents of IL-10, IL-12, iNOS, and TNF- α were detected using IL-10 (KET6019, Abbkine), IL-12 (KET6020, Abbkine), iNOS (ab253217, Abcam) and TNF- α (KET6032, Abbkine) kits, respectively.

Phagocytosis test

Totally 400,000 HCCLM3 cells labeled by CFSE (21888, Sigma) were seeded in ultra-low-attached 24-well plates (CLS3473-24EA, Corning Incorporated, Corning, NY) in presence of 200,000 macrophages treated with siNC-TCM or siCD38-TCM for 2-h incubation at 37°C. The co-cultured cells were collected and the proportion of CD11b⁺CFSE⁺ cells in total CD11b⁺ cells was analyzed by FACS and used for phagocytosis test.

CCK-8 assay

HCCLM3 cells were seeded into 96-well plates (1×10^5 cells/well), and the culture supernatant of HCCLM3 cells treated with siNC-TCM and siCD38-TCM (siNC-TCM-CM and siCD38-TCM-CM) was harvested and used to treat HCC cells for 24 h, 48 h and 72 h. Afterward, 10 μ L CCK-8 solution (CK04, Dojindo) was added to each well and incubated for 2 h. Subsequently, the OD values at 450 nm were measured using a microplate reader.

Transwell assay

HCCLM3 cells following treatment with siNC-TCM-CM or siCD38-TCM-CM were suspended in serum-free medium and seeded in 24-well plates of Transwell chamber (8 μ m, 3422, Corning) without Matrigel (CLS354277, Corning) at a density of 10,000 cells/well. The transwell chamber for the cell invasion experiment was pre-coated with Matrigel before the experiment. The serum-containing medium was added to the lower chamber. After 24 h, the cells were fixed in 4% paraformaldehyde, stained with 0.1% crystal violet, photographed under an optical microscope (E200, Nikon) and counted manually.

Isolation and identification of EVs

Mouse BM-MSCs (CP-M131, Procell) were cultured in complete medium. EVs were isolated from BM-MSC culture medium by differential centrifugation.¹⁶

The morphology of the isolated EVs was then observed under a TEM (H-7650, Hitachi Chemical, Tokyo, Japan). Western blot analysis was conducted to determine the expression of EV surface marker proteins (CD9 [ab92726, 1:2000, Rabbit, Abcam], CD63 [ab217345, 1:1000, Rabbit, Abcam] and calnexin [ab133615, 1:2000, Rabbit, Abcam]). NTA with NanoSight LM10 instrument (NanoSight Ltd., Minton Park, UK) was adopted to measure the size distribution of EVs.

Preparation of EVs/siCD38

Gene Pulser X Cell Electroporation System was used to load CD38 siRNA in BM-MSC-EVs by electroporation. EVs with a total protein concentration of 20 μ g were mixed with 20 μ g of CD38 siRNA in 400 μ L PBS (pH 7.3). Electroporation (square wave) was then conducted three times at 400 V and 125 μ F with the electric shock cup set at 0.4 cm, the pulse width set at 30 ms with a 2-second pause in-between. Afterward, the sample was immediately transferred to ice. Ultra-centrifugation was performed at 100000 \times g for 1 h to remove unloaded CD38 siRNA, and the supernatant was discarded. The precipitated EVs were resuspended, and the final BM-MSC-EVs loaded with CD38 siRNA were called EVs/siCD38.

Delivery efficiency Of EVs/siCD38 and EVs uptake assay

HCCLM3 cells were seeded in 12-well plates (1×10^5 cells/well) and cultured in an incubator with 5% CO₂ at 37°C for 24 h. FAM-siCD38 was loaded into EVs as previously described.

EVs/siCD38 was added to cells for incubation for 4 h at 37°C. The medium was renewed and cells continued to culture for another 20 h, followed by cell collection. FAM-positive cells were analyzed by flow cytometry to calculate the delivery efficiency of EVs to siCD38.

Initially, EVs or EVs/siCD38 was added with 5 μ M Dil dye (C1991S, Beyotime) for 15-min incubation at ambient temperature, and centrifuged at 1000 \times g for 5 min, with the supernatant removed. Next, EVs culture medium was added for resuspension, followed by centrifugation at 1000 \times g for 5 min and supernatant removal. These procedures were repeated twice and the obtained precipitate was the Dli-labeled EVs. Cover glasses were put on the top of the petri dish, where HCCLM3 cells were cultured. Upon reaching 50% confluence, the cells were co-cultured with Dli-labeled EVs or EVs/siCD38 at 37°C. After 24 h, the glasses were taken out, washed thrice with PBS, and soaked in 4% paraformaldehyde for 30 min at ambient temperature. Thereafter, the cells were permeabilized with 2% Triton X-100 for 15 min and stained with DAPI (2 μ g/mL, C1005, Beyotime) for 10 min. Finally, the expression of fluorescence was detected with an upright fluorescence microscope.

Xenograft tumor in mice

A total of 42 female C57BL/6 mice (5–6 weeks old) were housed under specific pathogen-free conditions at 26–28°C with 50–65% humidity. Animal experiments were ratified by the Animal Ethics Committee of The First Affiliated Hospital of Nanchang University. Mouse HCC cells Hepa1-6 were injected to the right armpit of the mice and 1 week later, EVs or EVs/siCD38 (100 μ g/mouse, once every other day, $n = 6$) were injected around the tumor of mice. Tumor volume was measured once every other day and calculated as follows: $W = 1/2 \times a \times b^2$ (a is the length and b is the width). Tumor was taken out after 24 days and used for subsequent analysis.

For PD-1/PD-L1 inhibitor resistance experiments, Hepa1-6 cells were inoculated into the right armpit of the mice and 1 week later, the mice was intraperitoneally injected with 200 μ g anti-PD-L1 (A1645, ABclonal) and its control IgG (A19711, ABclonal), once every other day, for 8 weeks as well as 200 μ L PBS or 200 μ L PBS containing 100 μ g EVs or 200 μ L PBS containing 100 μ g EVs/siCD38 surrounding the tumor using a 0.25 mL syringe (once a week, $n = 6$). No inflammatory reaction occurred surrounding the tumor. Tumor volume was measured once a week and calculated. After 8 weeks, the tumors were taken for follow-up experiments.

Identification of murine macrophages by FACS

Mouse tumor tissues were added with 5–10 mL HBSS + Ca/Mg (PB180323, Procell) + 10 μ g/mL DNase I (10104159001, Sigma-Aldrich) + 25 μ g/mL Liberase (5401054001, Roche), detached at 37°C for 30 min and vortexed once every 10 min. After lysis, the tumor suspension was filtered with a 70 m filter, placed on ice, washed with pre-cooled PBS, and centrifuged at 4°C and 1000 \times g for 5 min. Blood cells were lysed in ACK lysis buffer (A1049201, Invitrogen) for 10 min, which was halted by PBS, followed by centrifugation at 4°C and 1000 \times g for 5 min.

The samples were resuspended in FACS buffer, blocked with rat serum IgG (1 μ g/10⁶ cells, I4131-10 MG, Sigma-Aldrich) for 15 min and incubated with the following antibodies (all from BD Bioscience): BV480-TCR β (746385), FITC-CD11b (561688), PE-F4/80 (565410), Alexa Fluor[®] 647-CD206 (565250) and APC-CD80 (560016). For all channels, the positive and negative cells were gated on the basis of the FMOs.

Macrophage panel:

M1 macrophages: Hoechst-, TCR β -, CD11b+, F4/80+, CD80+ and CD206-.

M2 macrophages: Hoechst-, TCR β -, CD11b+, F4/80+, CD80-, and CD206 + .

Statistical analysis

Statistical analysis was completed applying SPSS 21.0 statistical software. Measurement data are expressed as mean \pm standard deviation. Data obeyed normal distribution and homogeneity of variance. Comparison between HCC tissues and adjacent normal tissues was implemented using paired t test, and independent sample of two groups was tested by un-paired t test. Comparison among multiple groups was assessed by one-way analysis of variance (ANOVA), followed by Tukey's post hoc tests. Two-way ANOVA was used for cell viability analysis, and repeated measures ANOVA was used for experimental tumor data. $p < .05$ indicates statistically significant difference.

Results

CD38 is highly expressed in the HCC tissues and cell lines

In total, 2 gene expression profile datasets of HCC tissue samples were retrieved from GEO database, namely GSE84005 ($n = 38$) and GSE174570 ($n = 57$). The batch effect was removed using ComBat function of the R “sva” software package. It was found that the data was randomly distributed without an intersection before the removal of bath effect (Figure 1a), while data was more evenly distributed with the bath effect removed (Figure 1b), highly suggestive of good correction effect. Based on the merged dataset, 328 genes significantly correlated with PD-L1 (CD274) were (Supplementary Table 4). Furthermore, CTD database yielded 940 HCC-related genes (Inference Score >90) (Supplementary Table 5). Moreover, 3288 genes related to HCC (Gifts >40) and 1900 genes related to tumor immunity (Gifts >40) were selected from GeneCards database (Supplementary Table 6, 7). Ten candidate genes were identified in the intersection of the above results, namely IFNG, PRKCB, CCND2, STAT1, MMP9, CD38, TAP1, CCL5, CASP1 and CXCL10 (Figure 1c). Protein-protein interaction (PPI) analysis of the encoding proteins is shown in Figure 1d. Of note, anti-CD38 and blocking PD-1/PD-L1 pathway have been reported to improve immunosuppression in tumor microenvironment,^{17,18} yet the functional role of CD38 in immunotherapy against HCC remains under-studied.

The results of reverse transcription quantitative polymerase chain reaction (RT-qPCR) and immunohistochemistry (IHC) showed an enhancement in CD38 expression in HCC tissues (Figure 1e, f). Higher expression of CD38 was also detected in human HCC cells (HCCLM3, Huh-7, and MHCC97-L)

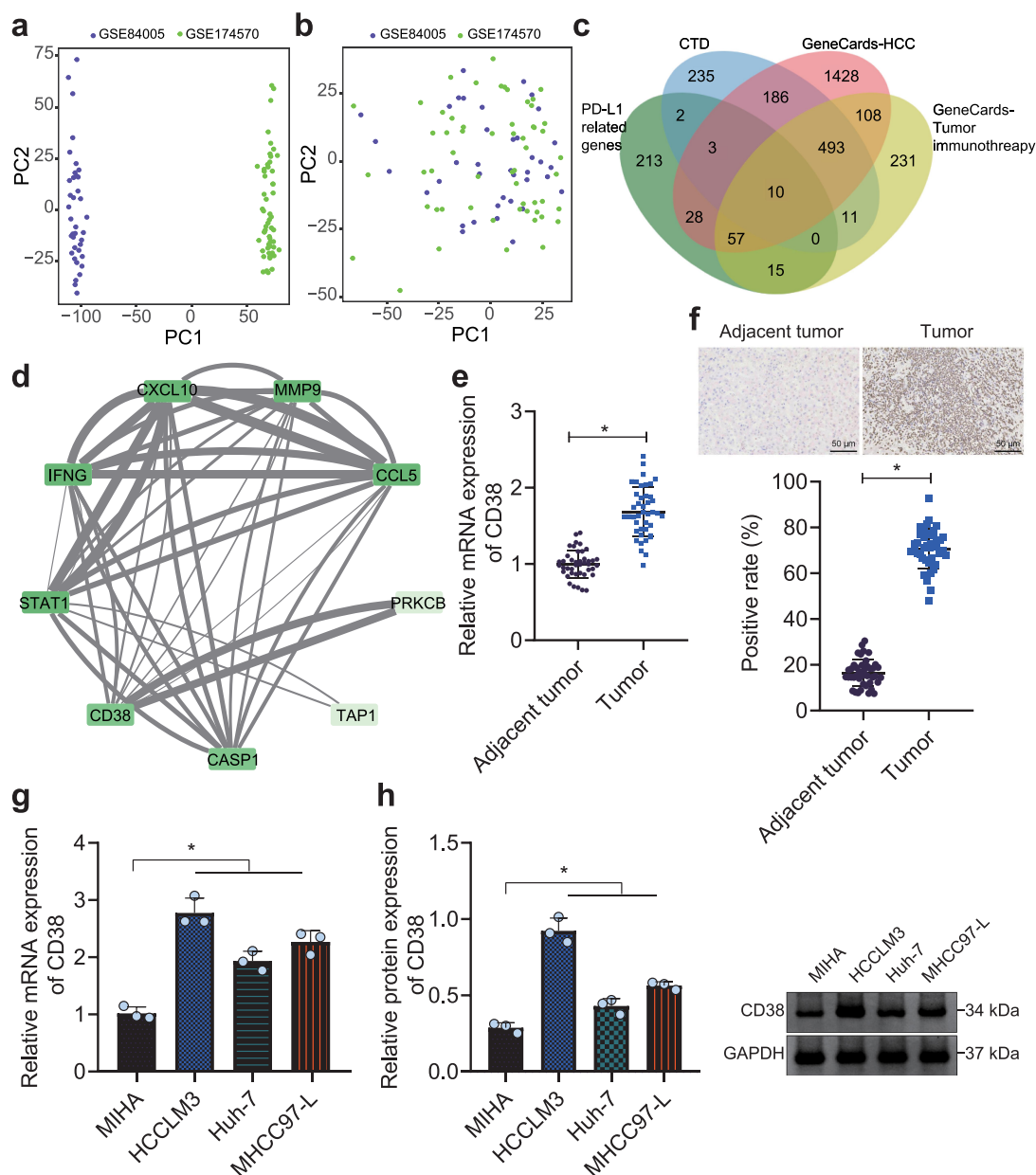


Figure 1. Amplified expression of CD38 expression in HCC. A, Data distribution of 2 expression profile datasets before the removal of batch effect. B, Data distribution of 2 expression profile datasets after the removal of batch effect. C, Venn diagram displaying the interaction of correlation analysis and screening results. D, Protein–protein interaction (PPI) analysis of candidate genes. Degree value indicates the number of PPI and decreases anticlockwise. The darker color represents higher Degree value. Combined score indicates the score of PPI. The thicker line represents larger Combined score. E, Expression of CD38 in HCC and adjacent normal tissues (n = 42) determined by RT-qPCR. F, Expression of CD38 in HCC and adjacent normal tissues (n = 42) determined by IHC, scale bar: 50 μ m. G, mRNA expression of CD38 in HCC cells (HCCLM3, Huh-7 and MHCC97-L) and human normal hepatocytes (MIHA) determined by RT-qPCR. H, Protein expression of CD38 in HCC cells (HCCLM3, Huh-7 and MHCC97-L) and human normal hepatocytes (MIHA) determined by Western blot analysis. * $p < .05$. The data in the figure are all measurement data, and expressed as mean \pm standard deviation. Comparison of adjacent normal tissues and HCC tissues was conducted by paired t test, and the comparison among multiple groups by one-way ANOVA. Cell experiments were repeated three times independently.

relative to that in human normal hepatocyte MIHA with HCCLM3 cells showing the highest expression (Figure 1g, h) and thus used for subsequent experimentations. The above results indicated highly expressed CD38 in HCC. Therefore, CD38 was selected for further investigation to explore the action of CD38 in the immunosuppression of HCC via the PD-1/PD-L1 signaling pathway with the aim to provide novel clinical immunotherapies for HCC.

Downregulation of CD38 promotes macrophage phagocytosis by inhibiting the adenosine receptor pathway, thus inhibiting the growth and metastasis of HCC cells

We then aimed to investigate the molecular mechanism of CD38 involved in HCC immunosuppression. It was evident that the expression of CD38 was found to be decreased in HCCLM3 cells treated with siCD38-1 or siCD38-2, with siCD38-2 exhibiting the superior silencing efficiency and thus

selected for subsequent experimentations (Figure 2a, b). CD38 enzyme activity was significantly downregulated after inhibition of CD38 expression by siCD38 (Figure 2c). Culture medium of siNC- and siCD38-treated HCCLM3 cells without erythro-9-(2-hydroxyl-3-nonyl)adenine (EHNA) intervention showed gradually degraded adenosine and no accumulation, with no significant difference, while upon EHNA, adenosine accumulated in the medium and its content was decreased in response to siCD38 at different time points (6 h, 12 h, 18 h, and 24 h) (Figure 2d, Supplementary Fig. 1A). This showed that CD38 silencing reduced adenosine production.

As depicted in Figure 2e-g, treatment with EHNA in THP-1 cells increased the expression of M2 macrophage markers IL-10 and ARG1 but reduced that of M1 macrophage markers IL-12, iNOS, and TNF- α . No significant difference was noted in M1 macrophage and M2 macrophage polarization in THP-1 cells between siNC and siCD38 transfection. In the presence of siCD38 + EHNA, the expression of IL-10 and ARG1 was reduced and that of IL-12, iNOS, and TNF- α was increased. These results suggested that CD38 silencing inhibited the adenosine receptor pathway to promote M1 polarization of macrophages.

Figure 2h shows the schematic diagram of experimental operation flow. Furthermore, macrophage phagocytosis was promoted in HCCLM3 cells with siCD38 (Figure 2j). Functional assays suggested that siCD38-TCM-CM inhibited the proliferative, migrative and invasive properties of HCCLM3 cells (Figure 2j, k, Supplementary Fig. 1B, C). In conclusion, siRNA-mediated CD38 silencing blocked adenosine receptor signaling to promote macrophage M1 polarization and then inhibit HCC cell growth and metastasis.

Preparation and identification of EVs/siCD38

EVs derived from bone marrow mesenchymal stem cells (BM-MSC-EVs) were isolated, and loaded with EVs/siCD38 by electroporation. TEM observation results showed that the isolated EVs and EVs/siCD38 were round or exhibited oval membranous vesicles (Figure 3a). Additionally, nanoparticles tracking analysis (NTA) results suggested that the diameter of EVs was 4–120 nm (Figure 3b). Western blot analysis results presented that CD63 and CD9 were expressed in the EVs and EVs/siCD38 but calnexin was hardly expressed (Figure 3c). The above results validated the successful isolation of EVs/siCD38. Western blot analysis results revealed a decline in the expression of CD38 in the presence of EVs/siCD38-1 or EVs/siCD38-2, with the EVs/siCD38-2 showing a more pronounced decline (Supplementary Fig. 2) and used for the subsequent experimentations.

Then, Dil-labeled EVs/siCD38 was co-cultured with HCCLM3 cells for 24 h. Dil-labeled EVs/siCD38 showed red fluorescence, and FAM labeled siCD38 showed green fluorescence. The laser confocal microscopic observation results showed that EVs/siCD38 was internalized by HCCLM3 cells and delivered siCD38 to HCCLM3 cells (Figure 3d). Besides, CD38 expression was reduced in HCCLM3 cells treated with EVs/siCD38 (Figure 3e), indicating that EVs/siCD38 was effectively internalized by HCC cells and inhibited CD38 expression in cells.

EVs/siCD38 inhibits tumor growth in mice

We further investigated the effect of EVs/siCD38 on tumor cells in mice. Higher CD38 expression was detected in Hepa1-6 cells than that in BNL 1ME A.7 R.1 cells (Figure 4a). Following injection of Hepa1-6 cells and EVs or EVs/siCD38, we found that tumor volume and weight were decreased in mice treated with EVs/siCD38 (Figure 4b, c). IHC results further verified that the expression of CD38 and Ki-67 was significantly reduced in the tumor tissues of EVs/siCD38-treated mice (Figure 4d). The above results indicated that EVs/siCD38 significantly inhibited tumor growth in mice.

For immunoregulation determination, EVs/siCD38 was found to lower the adenosine content, and the proportion of F4/80+/CD206+ cells while increasing the proportion of F4/80+/CD80+ cells (Figure 4e, f). Overall, EVs/siCD38 activated the tumor immune microenvironment by blocking the adenosine receptor pathway and inhibited tumor growth *in vivo*.

CD38 expression is upregulated in the HCC cell-bearing mice with the resistance to PD-1/PD-L1 inhibitor

We constructed anti-PD-L1-treatment-resistant mouse models by long-term injection of anti-PD-L1 antibody to tumor-bearing mice. From the 3rd week, tumor volume of mice was decreased following anti-PD-L1 treatment relative to that following IgG treatment. From the 5th week, the difference of tumor volume was decreased in the IgG- and anti-PD-L1-treated mice, with no significant difference at the 7th week (Figure 5a), indicating that the mice showed progressive resistance at the 5th week after anti-PD-L1 treatment. RT-qPCR and IHC results presented increased CD38 expression in the tumor tissues of mice resistant to anti-PD-L1 treatment (Figure 5b, c). Adenosine content was increased and the proportion of F4/80+/CD206+ cells was higher than that of F4/80+/CD80+ cells in response to resistance to anti-PD-L1 (Figure 5d, e). In conclusion, CD38 expression was upregulated, and the macrophage M2 polarization was increased in the mice resistant to PD-L1 blockade.

EVs/siCD38 reverses the resistance to PD-1/PD-L1 inhibitor in mice

Finally, we attempted to elucidate the effect of EVs/siCD38 on the resistance to PD-1/PD-L1 inhibitor in mice. No difference was noted in the tumor volume and weight of mice treated with PBS + anti-PD-L1 and EVs + anti-PD-L1. Tumor volume and weight were reduced in anti-PD-L1-treated mice after injection of EVs/siCD38 (Figure 6a, b). The results of IHC analysis showed no changes in the CD38 and Ki-67 expression in the tumor tissues of mice treated with PBS + anti-PD-L1 and EVs + anti-PD-L1. However, there was a decline in the CD38 and Ki-67 expression in the presence of EVs/siCD38 + anti-PD-L1 (Figure 6c). Additionally, no evident alterations were found in the adenosine content and macrophage polarization upon treatment with PBS + anti-PD-L1 and EVs + anti-PD-L1. Conversely, the adenosine content along with the proportion of F4/80+/CD206+ cells was decreased and the proportion of F4/80+/CD80+ cells was increased in response to treatment

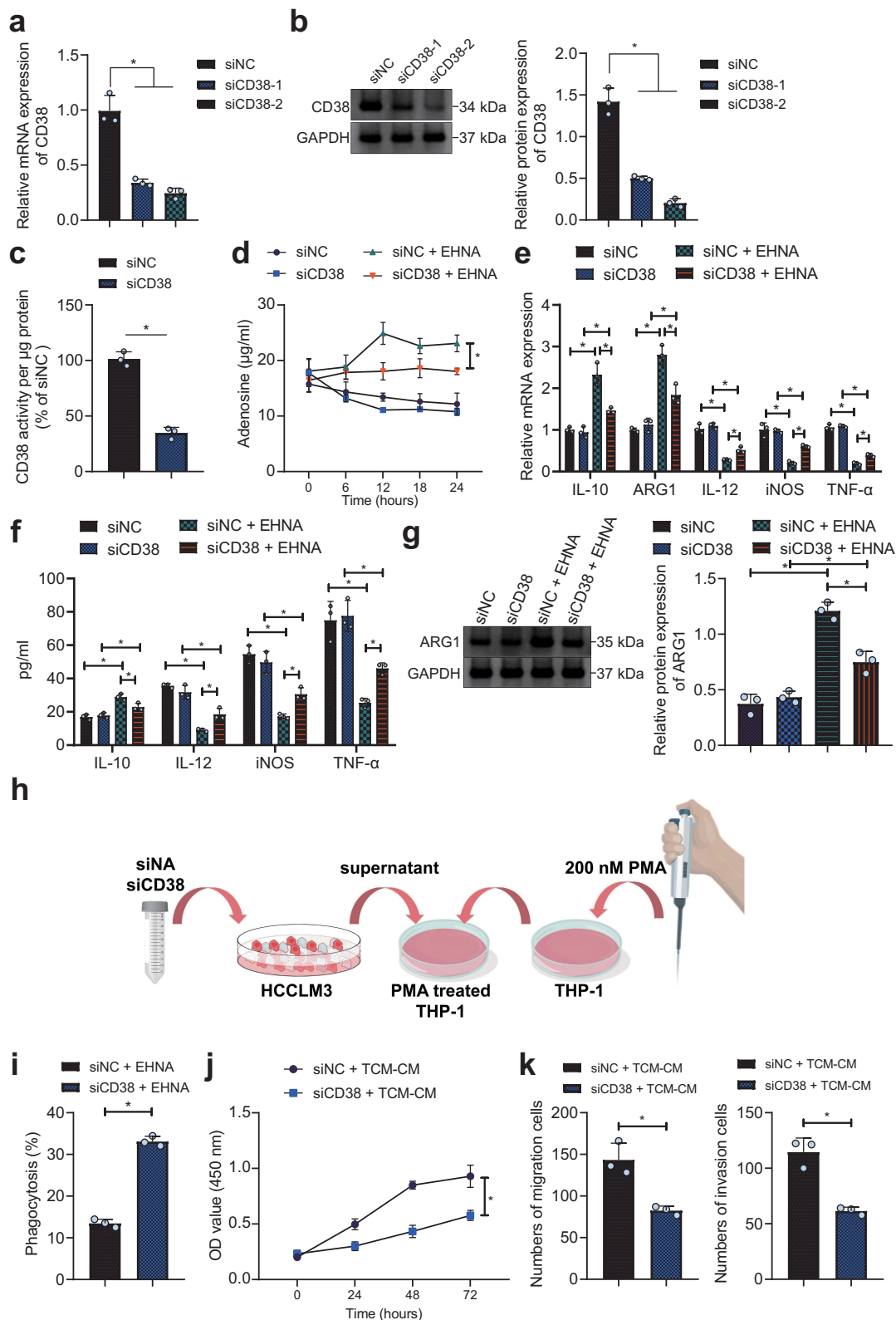
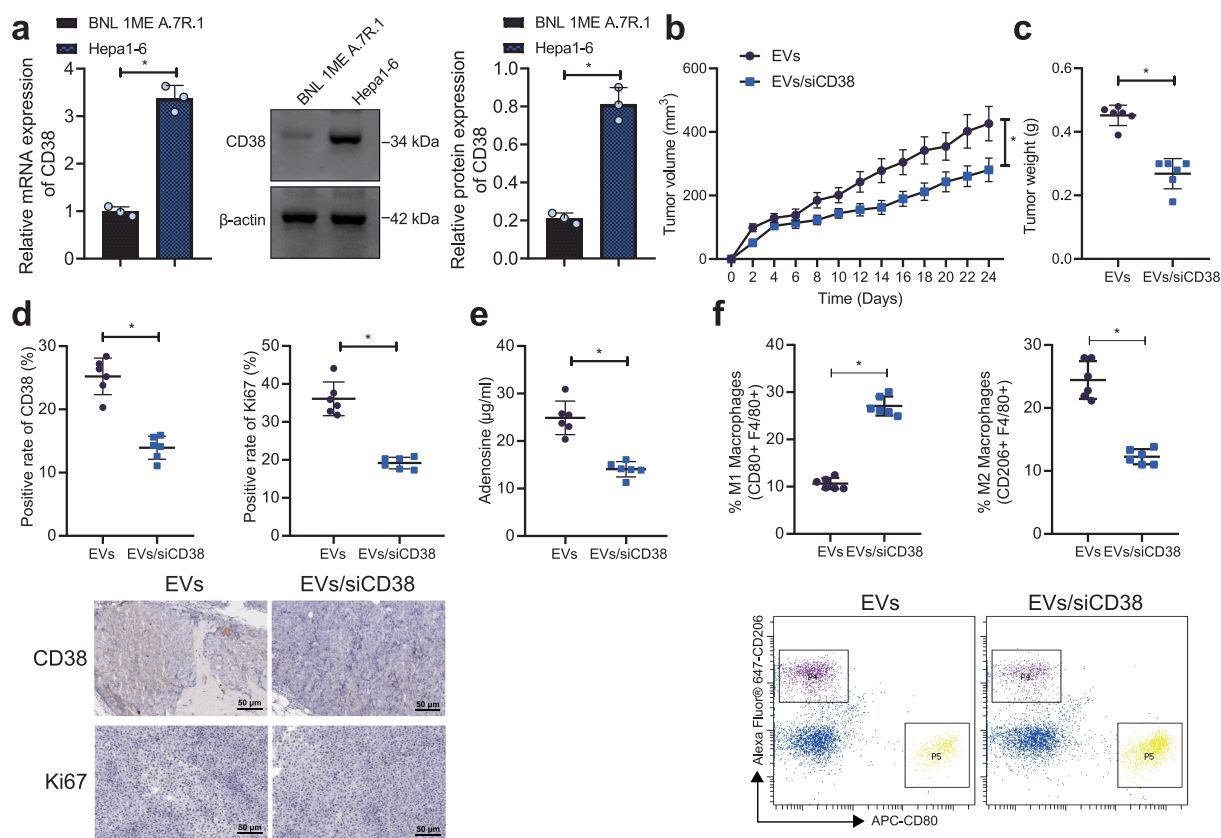
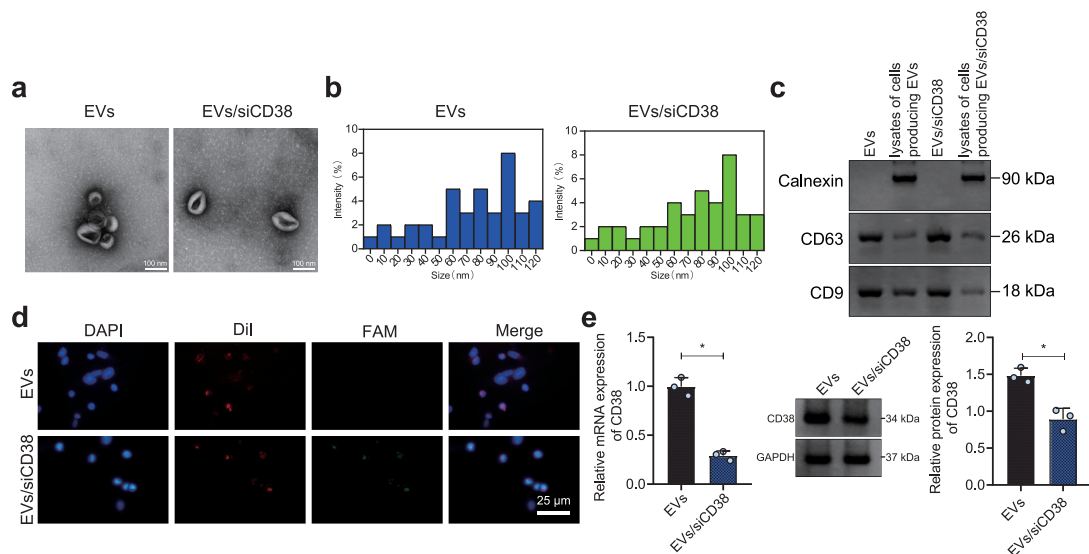


Figure 2. siRNA-mediated CD38 silencing induces M1 polarization of macrophages and arrests HCC cell growth by inhibiting adenosine receptor signaling.

A, Silencing efficiency of siCD38-1 and siCD38-2 determined by RT-qPCR in HCCLM3 cells. B, Silencing efficiency of the siCD38-1 and siCD38-2 detected by Western blot analysis in HCCLM3 cells. C, Enzyme activity of CD38 in HCCLM3 cells with siCD38. HCCLM3 cells were treated with siCD38 or combined with EHNA. D, Adenosine production in HCCLM3 cells. E, Determination of expression of M2 and M1 macrophage markers in THP1 exposed to conditioned media from HCCLM3 cells knocked-down or not by anti-CD38 siRNAs by RT-qPCR. F, Determination of expression of M2 and M1 macrophage markers in THP1 exposed to conditioned media from HCCLM3 cells knocked-down or not by anti-CD38 siRNAs by ELISA. G, THP-1 macrophage polarization after treatment with conditioned media from HCCLM3 cells knocked-down or not by anti-CD38 siRNAs determined by Western blot analysis. H, A schematic diagram to illustrate our experimental operation process. I, Macrophage phagocytosis after treatment with conditioned media from HCCLM3 cells knocked-down or not by anti-CD38 siRNAs determined by flow cytometry. J, HCCLM3 cell proliferation after THP1 exposed to conditioned media from HCCLM3 cells knocked-down or not by anti-CD38 siRNAs determined by CCK-8. K, HCCLM3 cell migration and invasion determined by Transwell assay. * $p < .05$. TCM-CM, the supernatant of HCCLM3 cell culture. The data in the figure are all measurement data, and are expressed as mean \pm standard deviation. Comparison of data in two groups was conducted by independent sample t test, and the comparison among multiple groups by one-way ANOVA. Cell proliferation at different time points was analyzed by two-way ANOVA. Cell experiments were repeated three times independently.



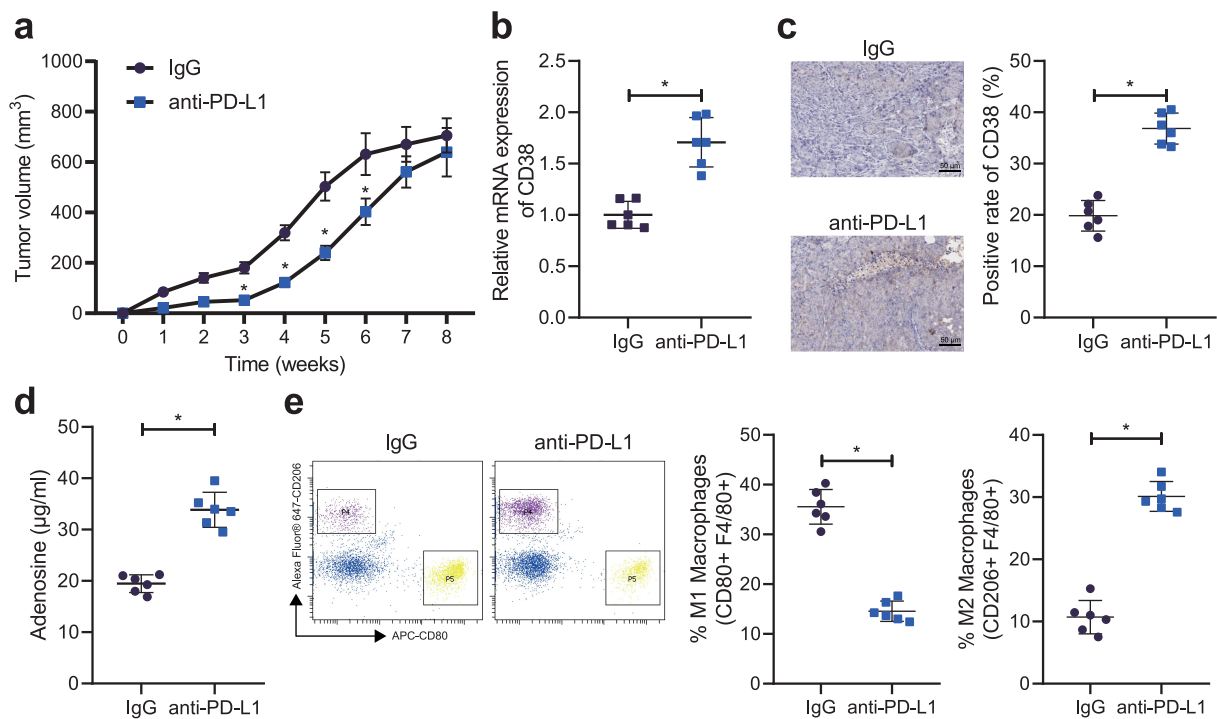


Figure 5. CD38 expression and macrophage M2 polarization are enhanced in the HCC cell-bearing mice resistant to PD-1/PD-L1 inhibitor. A, Measurement of the tumor volume of anti-PD-L1-treated mice. B, CD38 mRNA expression in the tumor tissues of mice resistant to anti-PD-L1 treatment detected by RT-qPCR. C, CD38 mRNA expression in the tumor tissues of mice resistant to anti-PD-L1 treatment detected by IHC, scale bar: 50 μ m. D, Adenosine content in the tumor tissues of mice resistant to anti-PD-L1 treatment detected by flow cytometry. E, Macrophage polarization in tumor tissues of mice resistant to anti-PD-L1 treatment detected by flow cytometry. $n = 6$, * $p < .05$. The data in the figure are all measurement data, and are expressed as mean \pm standard deviation. Comparison of data in two groups was conducted by independent sample t test. Data at different time points was analyzed by repeated measures ANOVA.

with EVs/siCD38 + anti-PD-L1 (Figure 6d, e). The above results indicated that EVs/siCD38 inhibited tumor growth *in vivo* by blocking the adenosine receptor pathway and activating the tumor immune microenvironment. Cumulatively, EVs/siCD38 reversed the resistance to PD-L1 blockade in mice, thus inhibiting tumor growth.

Discussion

The findings collected from our work provided evidence for the use of EVs-mediated delivery of CD38 siRNA to prevent immunosuppression feature of HCC and defined the mechanism underlying CD38-mediated HCC resistance to PD-1/PD-L1 inhibitor.

Our initial results depicted that CD38 was highly expressed in the HCC tissues and cell lines. Likewise, CD38 expression has been found to be increased in HepG2 cells.¹³ Subsequent findings of the current study indicated that BM-MSC-EVs were used as a delivery vector to deliver siCD38 into HCC cells. Indeed, EVs secreted by cells have been demonstrated to act as the delivery system to deliver gene therapeutic agents, including DNA and RNA to target cells, and adopt gene therapy strategies.¹⁹ Specifically, MSC-EVs loaded with PTEN siRNA limit the expression of PTEN in the injured spinal cord region after intranasal administrations and accelerate recovery for spinal cord injury individuals.²⁰

Previous study has documented that cell surface ectoenzymes, including CD38, modulate the generation of extracellular adenosine and therapeutic agents have been identified to

target adenosine and the adenosine receptor pathway for cancer immunotherapy as they both play a predominant role in anti-tumor immune cell responses.²¹ CD38-targeting antibodies can potentially limit the production of adenosine in the BM microenvironment, leading to improved T cell activity.²² Meanwhile, previous *in vitro* and *in vivo* data have clarified that CD38 blocks CD8 + T-cell function through the adenosine receptor pathway and that CD38 or adenosine receptor blockade effectively overcomes tumor cell immunosuppression.²³ At different stages of inflammatory response, macrophages mainly exhibit two subtypes: classically activated (M1) macrophages and the alternatively activated (M2) macrophages.²⁴ Decreased expression of IL-12, iNOS, and TNF- α indicates inhibition of macrophages polarized into M1 phenotype, while increased expression of IL-10 and ARG1 is predictive of M2 macrophage polarization; inhibiting the polarization of M2 macrophages results in suppression of HCC cell immune evasion, proliferation, invasion and migration.²⁵ Here, the present study revealed that silencing of CD38 combined with EHNA reduced the expression of IL-10 and ARG1 while increasing that of IL-12, iNOS, and TNF- α . Together with the previously reported, it can be concluded that EVs-mediated CD38 siRNA delivery polarizes macrophages toward M1 phenotype by inhibiting the adenosine receptor pathway, eventually delaying the immunosuppression, growth and metastasis of HCC.

Furthermore, the current results demonstrated that CD38 was upregulated in the HCC cell-bearing mice with the resistance to PD-1/PD-L1 inhibitor and EVs/siCD38 reversed the resistance to PD-1/PD-L1 inhibitor in mice. PD-L1(+) neutrophils from HCC

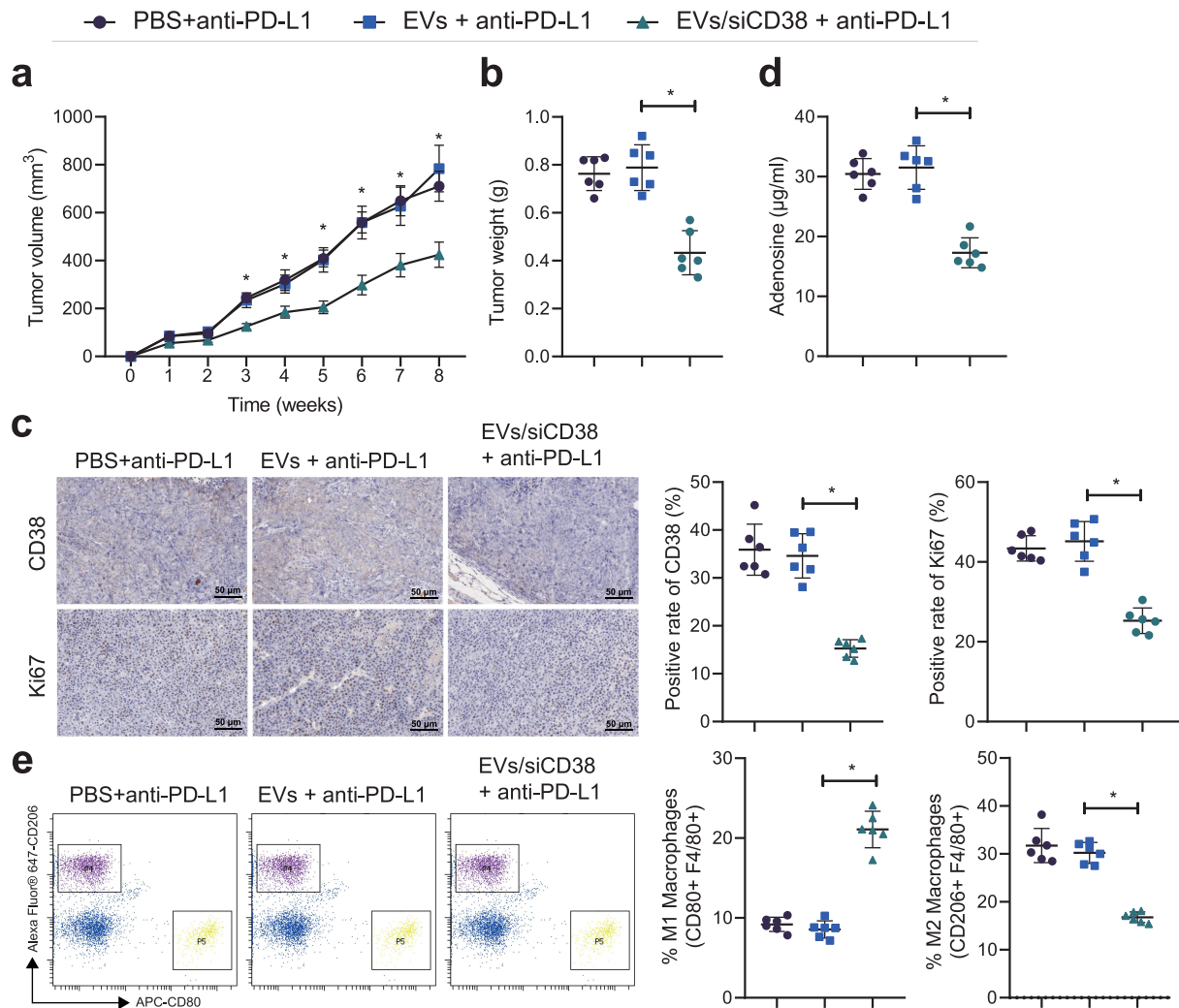


Figure 6. EVs/siCD38 abolishes the resistance to PD-L1 blockade and retards tumor growth in mice. Mice were treated with EVs + anti-PD-L1 or EVs/siCD38 + anti-PD-L1. A, Measurement of the tumor volume of mice. B, Measurement of the tumor weight of mice. C, CD38 and Ki-67 expression in the tumor tissues of mice detected by IHC, scale bar: 50 μ m. D, Adenosine content in the tumor tissues of mice. E, Macrophage polarization in tumor tissues of mice detected by flow cytometry. $n = 6$, * $p < .05$. The data in the figure are all measurement data, and are expressed as mean \pm standard deviation. Comparison of data in two groups was conducted by independent sample t test. Data at different time points was analyzed by repeated measures ANOVA.

patients are capable of blocking the activation of T cells, which can be partially reversed by the suppression of PD-L1.²⁶ Of note, the combination of dendritic cells pulsed with EVs derived from tumor cells and PD-1 antibody has been deciphered to improve the efficacy of sorafenib against HCC.²⁷ Moreover, a recent study has shown that tumors treated with anti-PD-1/PD-L1 antibodies can develop resistance, which is associated with the upregulation of CD38.²⁵ Recently, the CD38 metabolic pathways involving the immune-suppressive factor, adenosine, possibly exert critical roles in the possible mechanisms underlying the lack of responsiveness or resistance to anti-PD-L1/PD-1 antibodies.²⁸ Upregulation of CD38 increases the levels of extracellular adenosine and contributes to the resistance to anti-PD-1/PD-L1 therapy in the tumor microenvironment.²⁹ These reports supported the current findings that EVs-mediated CD38 siRNA delivery inhibited the adenosine receptor pathway and polarized macrophages toward M1 phenotype, eventually delaying the immunosuppression of HCC.

In the current investigation, we have revealed that CD38 altered the polarization of macrophages by affecting the accumulation of extracellular adenosine, thus causing the tumor immune-microenvironment to be immunosuppressed. However, so far we have not fully analyzed the types, numbers and distribution characteristics of immune cells in the HCC microenvironment. Other immune cells may also be directly regulated by CD38, such as CD8, Treg, etc. Therefore, further follow-up research is required for clinical application.

In conclusion, the current study demonstrated the antitumor efficacy of EVs/siCD38, which led to significantly decreased CD38 enzyme activity and adenosine secretion, yet promoted M1 polarization of macrophages and phagocytosis of HCC cells by macrophages, thereby reversing HCC resistance to PD-1/PD-L1 inhibitor (Figure 7). Such functional and biological changes contributed to the subsequent inhibition of HCC growth and metastasis. This rapid, cell-free and effective treatment holds great promise for the clinical use in HCC and beyond.

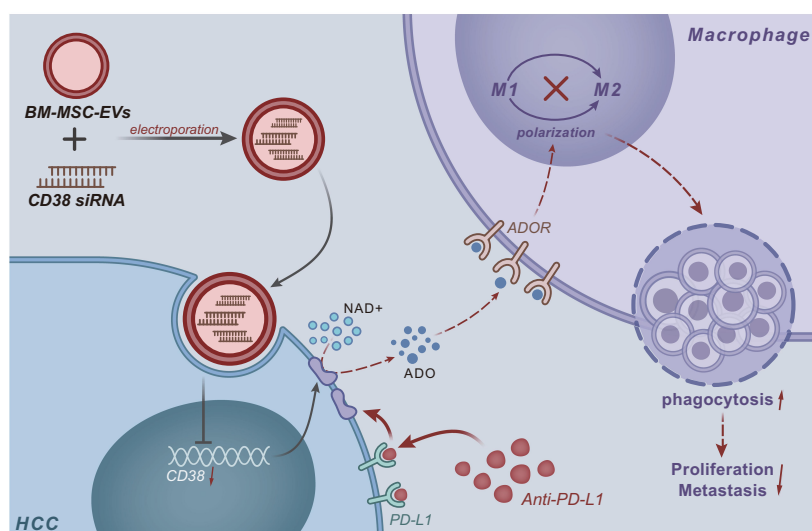


Figure 7. Schematic map of the role of EVs/siCD38 in HCC. The current study highlighted the antitumor efficacy of EVs/siCD38, which led to significantly decreased CD38 enzyme activity and adenosine secretion, yet promoted M1 polarization of macrophages and phagocytosis of HCC cells by macrophages, thereby reversing HCC resistance to PD-1/PD-L1 inhibitor.

Acknowledgments

Not applicable.

Disclosure statement

The authors declare that they have no competing interests.

Funding

The authors reported there is no funding associated with the work featured in this article.

Availability of data and materials

The datasets used and/or analyzed during the current study are available from the corresponding author on reasonable request.

Authors' contributions

JD designed the study. JD and HK collated the data, carried out data analyses and produced the initial draft of the manuscript. JD contributed to drafting the manuscript. All authors have read and approved the final submitted manuscript.

References

- Jee BA, Choi JH, Rhee H, Yoon S, Kwon SM, Nahm JH, Yoo JE, Jeon Y, Choi GH, Woo HG, et al. Dynamics of genomic, epigenomic, and transcriptomic aberrations during stepwise hepatocarcinogenesis. *Cancer Res.* 2019;79:5500–5512. doi:10.1158/0008-5472.CAN-19-0991.
- Villanueva A. Hepatocellular carcinoma. *N Engl J Med.* 2019;380:1450–1462. doi:10.1056/NEJMr1713263.
- Sperber AD, Bangdiwala SI, Drossman DA, Ghoshal UC, Simren M, Tack J, Whitehead WE, Dumitrascu DL, Fang X, Fukudo S, et al. Worldwide prevalence and burden of functional gastrointestinal disorders, results of Rome Foundation Global Study. *Gastroenterology.* 2021;160:99–114 e113. doi:10.1053/j.gastro.2020.04.014.
- Yang JD, Hainaut P, Gores GJ, Amadou A, Plymth A, Roberts LR. A global view of hepatocellular carcinoma: trends, risk, prevention and management. *Nat Rev Gastroenterol Hepatol.* 2019;16:589–604. doi:10.1038/s41575-019-0186-y.
- Buonaguro L, Mauriello A, Cavalluzzo B, Petrizzo A, Tagliamonte M. Immunotherapy in hepatocellular carcinoma. *Ann Hepatol.* 2019;18:291–297. doi:10.1016/j.aohep.2019.04.003.
- Pegtel DM, Gould SJ. Exosomes. *Annu Rev Biochem.* 2019;88:487–514. doi:10.1146/annurev-biochem-013118-111902.
- Barile L, Vassalli G. Exosomes: therapy delivery tools and biomarkers of diseases. *Pharmacol Ther.* 2017;174:63–78. doi:10.1016/j.pharmthera.2017.02.020.
- El-Andaloussi S, Lee Y, Lakhal-Littleton S, Li J, Seow Y, Gardiner C, Alvarez-Erviti L, Sargent IL, Wood MJ. Exosome-mediated delivery of siRNA in vitro and in vivo. *Nat Protoc.* 2012;7:2112–2126. doi:10.1038/nprot.2012.131.
- Dwivedi S, Rendon-Huerta EP, Ortiz-Navarrete V, Montano LF. CD38 and regulation of the immune response cells in cancer. *J Oncol.* 2021;2021:6630295. doi:10.1155/2021/6630295.
- Lam JH, HHM N, Lim CJ, Sim XN, Malavasi F, Li H, Loh JJH, Sabai K, Kim JK, Ong CCH, et al. Expression of CD38 on macrophages predicts improved prognosis in hepatocellular carcinoma. *Front Immunol.* 2019;10:2093. doi:10.3389/fimmu.2019.02093.
- HHM N, Lee RY, Goh S, Tay ISY, Lim X, Lee B, Chew V, Li H, Tan B, Lim S, et al. Immunohistochemical scoring of CD38 in the tumor microenvironment predicts responsiveness to anti-PD-1/PD-L1 immunotherapy in hepatocellular carcinoma. *J Immunother Cancer.* 2020;8:e000987. doi:10.1136/jitc-2020-000987.
- Gao L, Liu Y, Du X, Ma S, Ge M, Tang H, Han C, Zhao X, Liu Y, Shao Y, et al. The intrinsic role and mechanism of tumor expressed-CD38 on lung adenocarcinoma progression. *Cell Death Dis.* 2021;12:680. doi:10.1038/s41419-021-03968-2.
- Li S, England CG, Ehlerding EB, Kuttyreff CJ, Engle JW, Jiang D, Cai W. ImmunoPET imaging of CD38 expression in hepatocellular carcinoma using (64)Cu-labeled daratumumab. *Am J Transl Res.* 2019;11:6007–6015.
- Ke M, Zhang Z, Xu B, Zhao S, Ding Y, Wu X, Wu R, Lv Y, Dong J. Baicalein and baicalin promote antitumor immunity by suppressing PD-L1 expression in hepatocellular carcinoma cells. *Int Immunopharmacol.* 2019;75:105824. doi:10.1016/j.intimp.2019.105824.

15. Pathak R, Pharaon RR, Mohanty A, Villaflor VM, Salgia R, Massarelli E. Acquired resistance to PD-1/PD-L1 blockade in lung cancer: mechanisms and patterns of failure. *Cancers (Basel)*. 2020;12:3851. doi:10.3390/cancers12123851.
16. Zhou W, Zhou Y, Chen X, Ning T, Chen H, Guo Q, Zhang Y, Liu P, Zhang Y, Li C, et al. Pancreatic cancer-targeting exosomes for enhancing immunotherapy and reprogramming tumor microenvironment. *Biomaterials*. 2021;268:120546. doi:10.1016/j.biomaterials.2020.120546.
17. Zeng Y, Li B, Liang Y, Reeves PM, Qu X, Ran C, Liu Q, Callahan MV, Sluder AE, Gelfand JA, et al. Dual blockade of CXCL12-CXCR4 and PD-1/PD-L1 pathways prolongs survival of ovarian tumor-bearing mice by prevention of immunosuppression in the tumor microenvironment. *FASEB J*. 2019;33:6596–6608. doi:10.1096/fj.201802067RR.
18. Ogiya D, Liu J, Ohguchi H, Kurata K, Samur MK, Tai YT, Adamia S, Ando K, Hideshima T, Anderson KC. The JAK-STAT pathway regulates CD38 on myeloma cells in the bone marrow microenvironment: therapeutic implications. *Blood*. 2020;136:2334–2345. doi:10.1182/blood.2019004332.
19. Zhang Y, Bi J, Huang J, Tang Y, Du S, Li P. Exosome: a review of its classification, isolation techniques, storage, diagnostic and targeted therapy applications. *Int J Nanomedicine*. 2020;15:6917–6934. doi:10.2147/IJN.S264498.
20. Guo S, Perets N, Betzer O, Ben-Shaul S, Sheinin A, Michaelevski I, Popovtzer R, Offen D, Levenberg S. Intranasal delivery of mesenchymal stem cell derived exosomes loaded with phosphatase and tensin homolog siRNA repairs complete spinal cord injury. *ACS Nano*. 2019;13:10015–10028. doi:10.1021/acsnano.9b01892.
21. Sek K, Molck C, Stewart GD, Kats L, Darcy PK, Beavis PA. Targeting adenosine receptor signaling in cancer immunotherapy. *Int J Mol Sci*. 2018;19:3837. doi:10.3390/ijms19123837.
22. van de Donk N. Immunomodulatory effects of CD38-targeting antibodies. *Immunol Lett*. 2018;199:16–22. doi:10.1016/j.imlet.2018.04.005.
23. Chen L, Diao L, Yang Y, Yi X, Rodriguez BL, Li Y, Villalobos PA, Cascone T, Liu X, Tan L, et al. CD38-mediated immunosuppression as a mechanism of tumor cell escape from PD-1/PD-L1 blockade. *Cancer Discov*. 2018;8:1156–1175. doi:10.1158/2159-8290.CD-17-1033.
24. Lv R, Bao Q, Li Y. Regulation of M1 type and M2 type macrophage polarization in RAW264.7 cells by Galectin9. *Mol Med Rep*. 2017;16:9111–9119. doi:10.3892/mmr.2017.7719.
25. Liu W, Yu M, Xie D, Wang L, Ye C, Zhu Q, Liu F, Yang L. Melatonin-stimulated MSC-derived exosomes improve diabetic wound healing through regulating macrophage M1 and M2 polarization by targeting the PTEN/AKT pathway. *Stem Cell Res Ther*. 2020;11:259. doi:10.1186/s13287-020-01756-x.
26. He G, Zhang H, Zhou J, Wang B, Chen Y, Kong Y, Xie X, Wang X, Fei R, Wei L, et al. Peritumoural neutrophils negatively regulate adaptive immunity via the PD-L1/PD-1 signalling pathway in hepatocellular carcinoma. *J Exp Clin Cancer Res*. 2015;34:141. doi:10.1186/s13046-015-0256-0.
27. Shi S, Rao Q, Zhang C, Zhang X, Qin Y, Niu Z. Dendritic cells pulsed with exosomes in combination with PD-1 antibody increase the efficacy of sorafenib in hepatocellular carcinoma model. *Transl Oncol*. 2018;11:250–258. doi:10.1016/j.tranon.2018.01.001.
28. Costa F, Marchica V, Storti P, Malavasi F, Giuliani N. PD-L1/PD-1 axis in multiple myeloma microenvironment and a possible link with CD38-mediated immune-suppression. *Cancers (Basel)*. 2021;13:164. doi:10.3390/cancers13020164.
29. Mittal D, Vijayan D, Smyth MJ. Overcoming acquired PD-1/PD-L1 resistance with CD38 blockade. *Cancer Discov*. 2018;8:1066–1068. doi:10.1158/2159-8290.CD-18-0798.